REPORT DOCUMENTATION PAGE

Form Approved OMB NO. 0704-0188

The public reporting burden for this collection of information is estimated to average 1 hour per response, including the time for reviewing instructions, searching existing data sources, gathering and maintaining the data needed, and completing and reviewing the collection of information. Send comments regarding this burden estimate or any other aspect of this collection of information, including suggesstions for reducing this burden, to Washington Headquarters Services, Directorate for Information Operations and Reports, 1215 Jefferson Davis Highway, Suite 1204, Arlington VA, 22202-4302. Respondents should be aware that notwithstanding any other provision of law, no person shall be subject to any oenalty for failing to comply with a collection of information if it does not display a currently valid OMB control number.
PLEASE DO NOT RETURN YOUR FORM TO THE ABOVE ADDRESS.

1. REPORT DATE (DD-MM-YYYY)	2. REPORT TYPE	3. DATES COVERED (From - To)
15-08-2013	Conference Proceeding	-

4. TITLE AND SUBTITLE

Infrared Emitters and photodetectors with InAsSb bulk active region

5a. CONTRACT NUMBER

W911NF-12-2-0057

5b. GRANT NUMBER

5c. PROGRAM ELEMENT NUMBER

611102

6. AUTHORS

Ding Wang, Youxi Lin, Dmitry Donetsky, Gela Kipshidze , Leon Shterengas, Gregory Belenky, Stefan P. Svensson, Wendy L. Sarney, Harry Hier

5d. PROJECT NUMBER

5e. TASK NUMBER

5f. WORK UNIT NUMBER

7. PERFORMING ORGANIZATION NAMES AND ADDRESSES

Research Foundation of SUNY at Stony Brook U
Office of Sponsored Programs
W-5510 Melville Library
Stony Brook, NY 11794 -3362

8. PERFORMING ORGANIZATION REPORT NUMBER

9. SPONSORING/MONITORING AGENCY NAME(S) AND ADDRESS(ES)

U.S. Army Research Office
P.O. Box 12211
Research Triangle Park, NC 27709-2211

10. SPONSOR/MONITOR'S ACRONYM(S)

ARO

11. SPONSOR/MONITOR'S REPORT NUMBER(S)

62447-EL.4

12. DISTRIBUTION AVAILIBILITY STATEMENT

Approved for public release; distribution is unlimited.

13. SUPPLEMENTARY NOTES

The views, opinions and/or findings contained in this report are those of the author(s) and should not contrued as an official Department of the Army position, policy or decision, unless so designated by other documentation.

14. ABSTRACT

Bulk unrelaxed InAsSb alloys with Sb compositions up to 44% and layer thicknesses up to 3 um were grown by molecular beam epitaxy. The alloys showed photoluminescence (PL) energies as low as 0.12 eV at T=13K. The electroluminescence and quantum efficiency data demonstrated with unoptimized barrier heterostructures at T=80 and 150K suggested large absorption coefficient and carrier lifetimes sufficient for the development of long wave infrared photodetectors and emitters with high quantum efficiency. The minority hole transport was found to be

15. SUBJECT TERMS

metamorphic growth, InAsSb, quantum efficiency, long-wave infrared, barrier detector

16. SECURITY CLASSIFICATION OF:			17. LIMITATION OF ABSTRACT	15. NUMBER OF PAGES	19a. NAME OF RESPONSIBLE PERSON
a. REPORT	b. ABSTRACT	c. THIS PAGE			Gregory Belenky
UU	UU	UU	UU		19b. TELEPHONE NUMBER
					631-632-8397

Standard Form 298 (Rev 8/98)
Prescribed by ANSI Std. Z39.18

Report Title

Infrared Emitters and photodetectors with InAsSb bulk active region

ABSTRACT

Bulk unrelaxed InAsSb alloys with Sb compositions up to 44% and layer thicknesses up to 3 um were grown by molecular beam epitaxy. The alloys showed photoluminescence (PL) energies as low as 0.12 eV at T=13K. The electroluminescence and quantum efficiency data demonstrated with unoptimized barrier heterostructures at T=80 and 150K suggested large absorption coefficient and carrier lifetimes sufficient for the development of long wave infrared photodetectors and emitters with high quantum efficiency. The minority hole transport was found to be adequate for development of the detectors and emitters with large activer layer thickness.

Conference Name: SPIE Defense, Security+ Sensing

Conference Date: April 29, 2013

PROCEEDINGS OF SPIE

Infrared Technology and Applications XXXIX

Bjørn F. Andresen
Gabor F. Fulop
Charles M. Hanson
Paul R. Norton
Editors

29 April–3 May 2013
Baltimore, Maryland, United States

SPIE Defense, Security + Sensing

Volume 8704
Part One of Two Parts

SPIE

Infrared emitters and photodetectors with InAsSb bulk active regions

Ding Wang[a], Youxi Lin[a], Dmitry Donetsky[a], Gela Kipshidze[a], Leon Shterengas[a], Gregory Belenky[a], Stefan P. Svensson[b], Wendy L. Sarney[b], Harry Hier[b]

[a]Department of ECE, Stony Brook University, NY 11794, USA;
[b]U.S. Army Research Laboratory, 2800 Powder Mill Rd, Adelphi, MD 20783, USA

ABSTRACT

Bulk unrelaxed InAsSb alloys with Sb compositions up to 44 % and layer thicknesses up to 3 μm were grown by molecular beam epitaxy. The alloys showed photoluminescence (PL) energies as low as 0.12 eV at T = 13 K. The electroluminescence and quantum efficiency data demonstrated with unoptimized barrier heterostructures at T= 80 and 150 K suggested large absorption and carrier lifetimes sufficient for the development of long wave infrared detectors and emitters with high quantum efficiency. The minority hole transport was found to be adequate for development of the detectors and emitters with large active layer thickness.

Keywords: metamorphic growth, InAsSb, quantum efficiency, long-wave infrared, barrier detector

1. INTRODUCTION

Growth of $InAs_{1-x}Sb_x$–based epitaxial materials for infrared photodetectors has a long development history [1-2]. A strong energy gap bowing in these materials results in the smallest energy gaps available within the III-V semiconductor compounds. For bulk alloys with a particular composition the value of the energy gap is affected by growth conditions, which in turn influences the presence or absence of residual strain and/or group V ordering in the InAsSb layer. Many earlier publications reported the growth of relaxed InAsSb layers on various substrates [3-5]. Photoconductive detectors based on relaxed InAsSb grown on GaAs were demonstrated [6]. The relaxed InAsSb show high dislocation densities and relatively broad photoluminescence spectra [7-8].

In order to improve the optical quality of the material and to reduce the dislocation density, bulk InAsSb layers were grown on various types of strain-relieving, graded buffer layers that accommodate the difference between the lattice constants of the epitaxial layer and the substrate. Bulk InAsSb layers with a narrow PL spectrum were grown with $Al_{0.7}In_{0.3}Sb$/AlSb Strained Layer Superlattice (SLS) buffers on GaSb substrates [9]. By that time, 145 meV (λ = 8.6 μm) was reported to be the minimum energy gap for the bulk InAsSb alloys at 77 K. Observations of absorption at longer wavelengths, could only be found in ordered InAsSb alloys and InAsSb-based Strained Layer Superlattices (SLS). Low-temperature energy gaps of 132 meV and 117 meV were reported for ordered $InAsSb_{0.4}$ [9-10] and InAsSb-based SLS absorbers, respectively [11-12]. Using the strain-relief buffers, photovoltaic devices based on an InAsSb SLS absorber with $D^* = 1\times10^{10}$ cmHz$^{1/2}$/W at $\lambda \leq 10$ μm operating at T = 77 K were demonstrated [13].

Recently, the number of publications devoted to the development of InAsSb-based materials has increased [14-25]. With the demonstrated advantage of the barrier detectors [18-19], the mid-wave infrared detector industry's interest has turned toward heterostructure detectors with bulk InAsSb absorbers and AlSb-based barriers. These structures can outperform InSb homojunction photodetectors operating at elevated temperatures. InAsSb-based materials are also gaining attention for the development of long-wave infrared (LWIR) photodetectors. One of the reasons is a long minority carrier lifetime in undoped InAsSb-based materials [21-22] compared to that in InAs/GaSb SLS lightly doped with Beryllium [26-27].

Infrared Technology and Applications XXXIX, edited by Bjørn F. Andresen, Gabor F. Fulop, Charles M. Hanson, Paul R. Norton, Proc. of SPIE Vol. 8704, 870410 · © 2013 SPIE
CCC code: 0277-786X/13/$18 · doi: 10.1117/12.2016082

The relatively short electron lifetime in LWIR InAs/GaSb SLS can be explained with presence of deep recombination centers related to antisite and other defects [28-29].

The development of bulk InAsSb alloys with Sb compositions up to 44 % was demonstrated recently [21]. The materials were grown on GaSb substrates with two types of buffers, GaInSb and AlInSb, utilizing linear grading of the buffer composition. The InAsSb layers were grown with a lateral lattice constant equal to that of the top of the buffer resulting in a low residual strain (< 0.1%). Care was taken to avoid the formation of any natural SLS. Unstrained InAsSb alloys grown on graded buffer layers were found to have a random distribution of group V atoms (ordering-free) [23]. Analysis of electron diffraction patterns for InAsSb showed that ordering correlates with the presence of strain. The inherent energy gap for the bulk unstrained $InAsSb_{0.44}$ was found to be 120 meV at T = 13 K The nature of the strong bowing of the energy gap in InAsSb remains unclear, but it is not due to ordering or residual strain.

Minority carrier lifetimes up to 350 ns at T= 77 K were reported for 1-μm-thick undoped bulk $InAsSb_{0.2}$ layers grown on metamorphic buffers [30]. Even longer minority carrier lifetimes up to 9 μs at T = 77 K were reported for undoped InAsSb/InAs SLS pseudomorphically-grown on GaSb substrates [25]. InAsSb/InAs SLS-based barrier detectors with a cut-off wavelength of 13.2 μm and a modest quantum efficiency of 2.5 % at T = 77 K were demonstrated [31]. In the present work the growth of heterostructures consisting of bulk, strain-free InAsSb and barrier materials was pursued for long-wave infrared photodetectors and emitters with high quantum efficiency.

2. MATERIAL GROWTH AND CHARACTERIZATION

The heterostructures were grown on GaSb substrates by solid-source molecular beam epitaxy (MBE) utilizing valved crackers for As and Sb. The substrate temperature was controlled by pyrometer previously calibrated using references such as the III to V enriched surface reconstruction transition, oxide desorption and melting point of InSb. The growth temperature was maintained near 415 ^{0}C for the InAsSb layers. The growth rate was about 1 μm per hour. The Sb incorporation was adjusted by the relatives pressure of As and Sb as measured by a beam-flux-monitor. The compositionally graded buffer layers were up to 3.5 μm thick and grown at elevated temperatures ranging from 460 to 520 ^{0}C. In this work GaInSb buffer layers with linear composition grading were used with the lattice constant increase rate ranging from 0.5 to 0.8 % per micron. The native (without strain distortion) lattice constant of the top of the buffer was 1.2-1.3 % greater that the target lateral lattice constant. For GaInSb buffers this approach was implemented in Ref. 31.

The experimental results presented in this work were obtained with the bulk InAsSb materials with Sb compositions of 20 and 44 %. Most of the heterostructures had the thickness of InAsSb layers of 1 μm. The presented transmission electron microscopy (TEM) data were obtained for the 0.5-μm-thick InAsSb layers with 20 % Sb composition. The bulk InAsSb layers with 44 % Sb composition had the layer thicknesses of 1 and 3 μm. The InAsSb layers were undoped and showed n-type conductivity.

Figure 1 shows a cross-sectional (220) bright field TEM image of the $InAs_{0.8}Sb_{0.2}$ bulk layer grown on a GaInSb graded buffer. No dislocations can be seen in the epi-structure containing the $InAs_{0.8}Sb_{0.2}$ bulk layer. The long dislocation lines seen in the lower part of the buffer layers are aligned along the [110] direction, indicating efficient dislocation glide in the graded buffer. The topmost portion of the graded buffer remained unrelaxed under compressive strain. The bulk InAsSb layers were grown nearly lattice matched to the in-plane lattice constants of the topmost of the strained section of the buffers.

No evidence of long-range CuPt-type ordering was observed in electron diffraction patterns obtained with transmission electron microscopy [23].

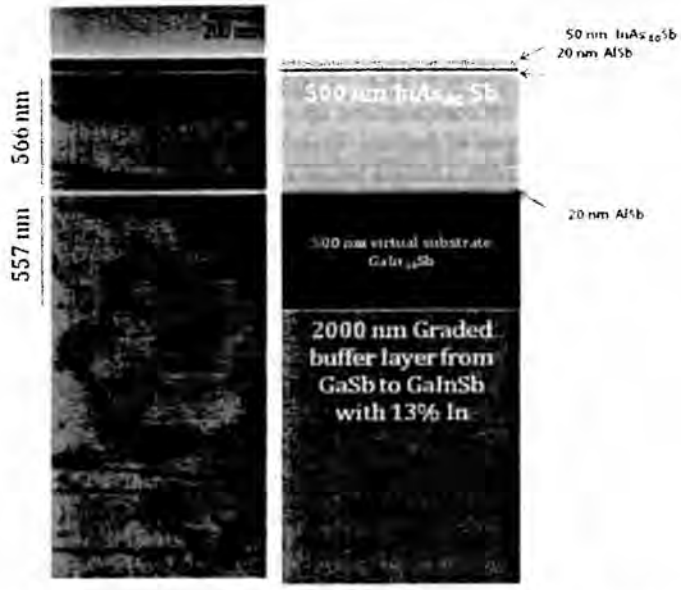

Figure 1. XTEM image (220 bright field with two beam condition) of the metamorphic structure with 0.5-μm thick $InAs_{0.8}Sb_{0.2}$ bulk layer grown on GaInSb graded buffer.

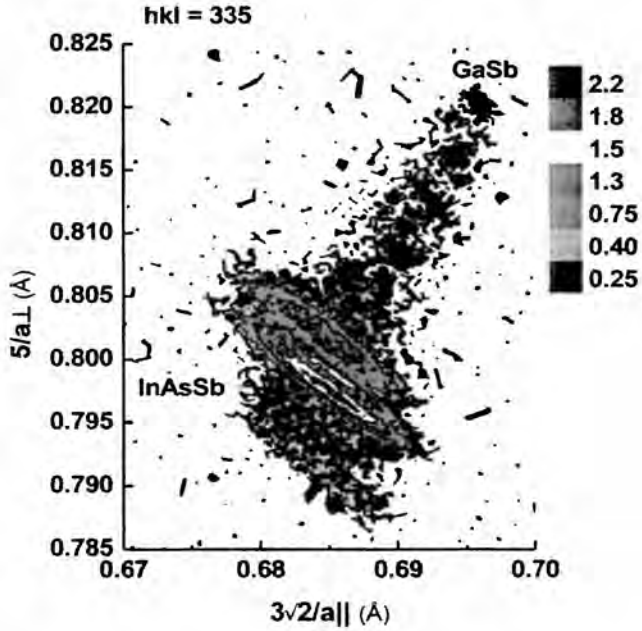

Figure 2. Asymmetric (335) RSM taken at azimuth angle equal to 90° for $InAsSb_{0.4}$ layer grown on the top of GaInSb buffer. The color bar shows the relative counts in logarithmic scale.

Asymmetric (335) Reciprocal Space Mapping (RSM) was used to determine the lateral lattice constant of the top portion of the buffer (Figure 2). The diagonal line starting from the substrate peak in the top right corner corresponds to the relaxed part of the buffer with a lattice parameter gradually increasing from that of GaSb. The peak in the center corresponds to InAsSb layer. The vertical line going down from the InAsSb peak reflexes the top strained section of the buffer grown pseudomorphically on the top of the relaxed buffer section.

The PL spectra were measured with a Fourier-transform infrared (FTIR) spectrometer. The responsivity spectrum of the liquid-nitrogen cooled HgCdTe detector extends to $\lambda = 14$ μm. The PL was excited by a 1064 nm solid-state laser and was collected by reflective optics. PL was observed in a wide temperature range, up to room temperature for structures with 20 % Sb and up to 250 K for those with 44 % Sb compositions [33].

The PL spectra were obtained with excitation powers of 100 mW. The excitation area was 1.2×10^{-3} cm^2. Figure 3 shows the normalized PL spectra of the bulk InAsSb alloys measured at T = 13 K. The energy gap values were determined from the PL peak maxima at T = 13 K. This simplified approach provided adequate accuracy for ternary materials.

The PL data obtained for recently grown InAsSb layers with large Sb compositions were used for updating the value of the bowing parameter reported in the earlier publication [21]. Fitting the dependence of the PL peak energy on Sb composition with data for older and recently grown bulk InAsSb (Figure 4) is consistent with the energy gap bowing parameter of 0.87 eV reported in [23, 33].

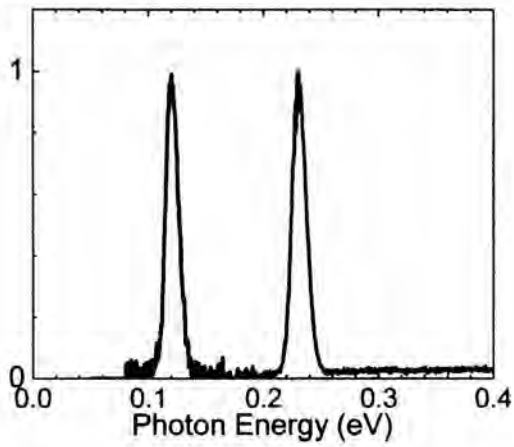

Figure 3. The normalized PL spectra for heterostructures with 1-μm thick InAsSb layers and Sb compositions of 20 % (red line) and 44 % (blue line) measured at T = 13 K.

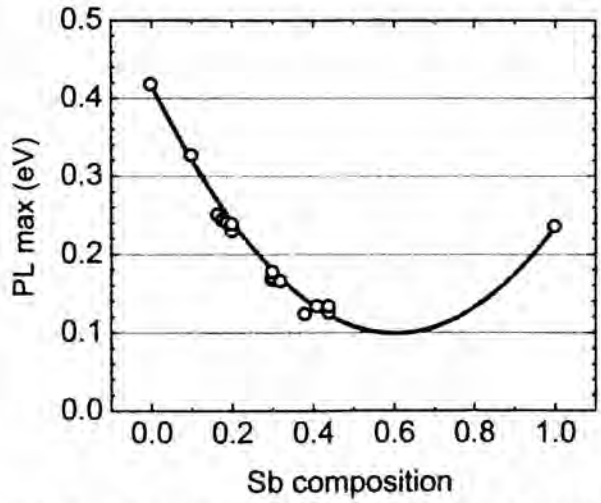

Figure 4. The dependence of PL peak energy versus Sb composition for bulk InAsSb measured at T=13 K. The best fit was obtained with the bowing parameter of 0.87 eV.

The fitting in Figure 4 suggests that bulk InAsSb alloys with higher than 44 % Sb compositions can have energy gaps even smaller than those reported in this work.

3. HETEROSTRUCTURES FOR STUDY OF THE ELECTROLUMINESCENCE

Strong PL from the bulk InAsSb materials observed up to room temperature indicated that the materials could be effective emitters of infrared radiation with electrical injection of carriers [34]. In order to assess the carrier transport properties, heterostructures incorporating undoped InAsSb layers were grown on n-doped GaSb substrates with GaInSb buffers doped with Tellurium. The energy bending at the interface of the GaInSb buffer and the InAsSb layer was serving as a barrier for the confinement of holes. To obtain electron confinement, a wide energy gap barrier comprising of 200-nm-thick p-doped AlInAsSb was grown on the top of bulk InAsSb layer. The composition of the quaternary barrier layer was chosen to match the lattice constants and to align the valence band of the barrier to that of the InAsSb layer. For the contact layer a p-doped InAsSb of the same composition as the bulk layer was grown on the top of the barrier. The contact layer was doped with Beryllium to a level of $p=1\times10^{19}$ cm^{-3}.

Figure 5 shows the schematic band diagram of the barrier heterostructure with a bulk $InAsSb_{0.2}$ layer for study of electroluminescence (EL). The heterostructures were processed as follows. A 300-nm-thick silicon nitride dielectric layer was deposited. Windows of 400-μm diameter were opened in the dielectric in which top Ti/Pt/Au metal contacts were deposited. The wafers were lapped down to a thickness of 200 μm. Ni/Au/Ge/Ni/Au metal contacts were deposited on the n-GaSb substrate and annealed followed by Ti/Pt/Au metallization. The heterostructures were cleaved into squares with a 600 μm side and soldered p-side down on copper heatsinks. EL was observed from the substrate side through a 500-μm diameter window in the metal contact. No antireflection coating was deposited.

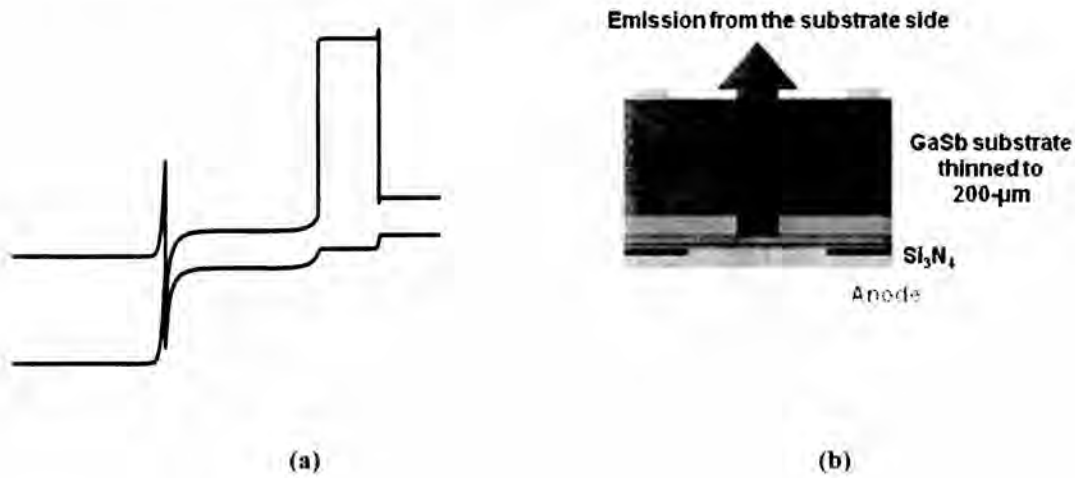

Figure 5. (a) The band diagram of the heterostructure with the undoped bulk $InAsSb_{0.2}$ layer grown on the Te-doped GaInSb buffer. The p-doped AlInAsSb electron confinement layer had a 200-nm thickness. The top p-contact layer consisted of 200 nm-thick InAsSb doped with Beryllium (1×10^{19} cm^{-3}) (b) The schematic cross-section of the processed heterostructures for study of electroluminescence.

The optical power was measured using calibrated InSb and HgCdTe photodetectors and an integrating sphere. The electroluminescence spectra were measured with an FTIR spectrometer.

Figure 6 shows the electroluminescence spectra and output power for heterostructures with a 1-μm-thick InAsSb layer with Sb composition of 20 %. The maximum output power levels of 90 μW and 10 μW were obtained at $\lambda \approx 5$ μm at T= 77 K and room temperature, respectively. Similar dependences for InAsSb heterostructures with 44 % Sb and active layer thicknesses of 1 and 3 μm are shown in Figure 7. Output power levels up to 8 μW were measured for 1-μm-thick heterostructure with 44 % Sb composition. The EL maximum was observed at $\lambda \approx 8$ μm. The blue shift of the EL energy peak compared to the PL peak at $\lambda \approx 10$ μm is explained by band filling under electrical injection.

A sublinear character of the dependences of output power on current for heterostructures with a 1-μm thick active layer can be explained by contribution of Auger recombination at high injection. A greater slope and linear dependence for a

3-μm-thick heterostructure indicate smaller contribution of Auger recombination due to smaller excess carrier concentration. This is strong evidence of the efficient hole transport in the bulk $InAsSb_{0.44}$ at T = 80 K. This encouraged further studies of the material for long wave infrared photodetectors.

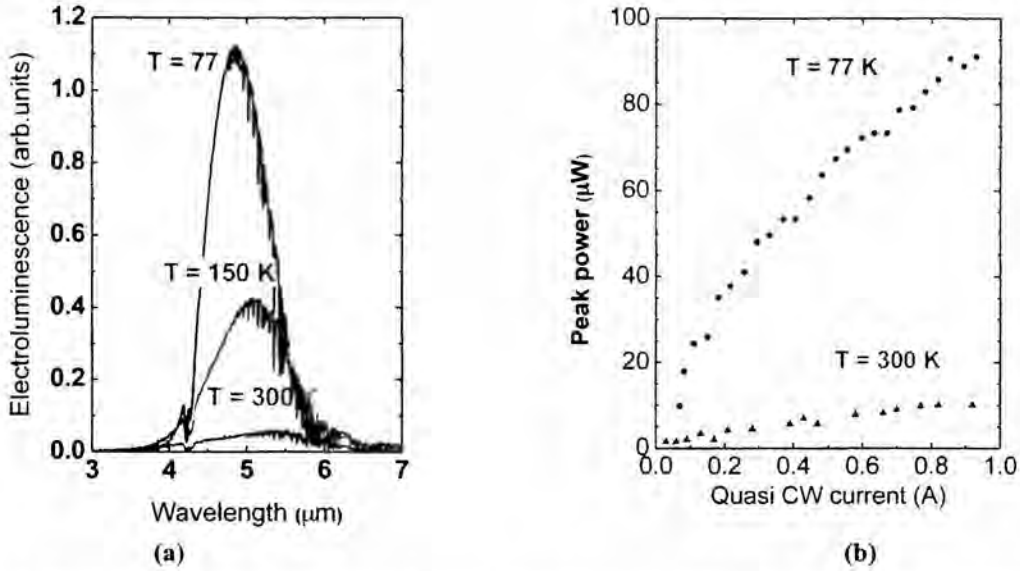

Figure 6. Electroluminescence spectra (a) and power dependences on current (b) for InAsSb heterostructures with 20 % Sb composition. The power dependences were measured with a 50 % duty cycle.

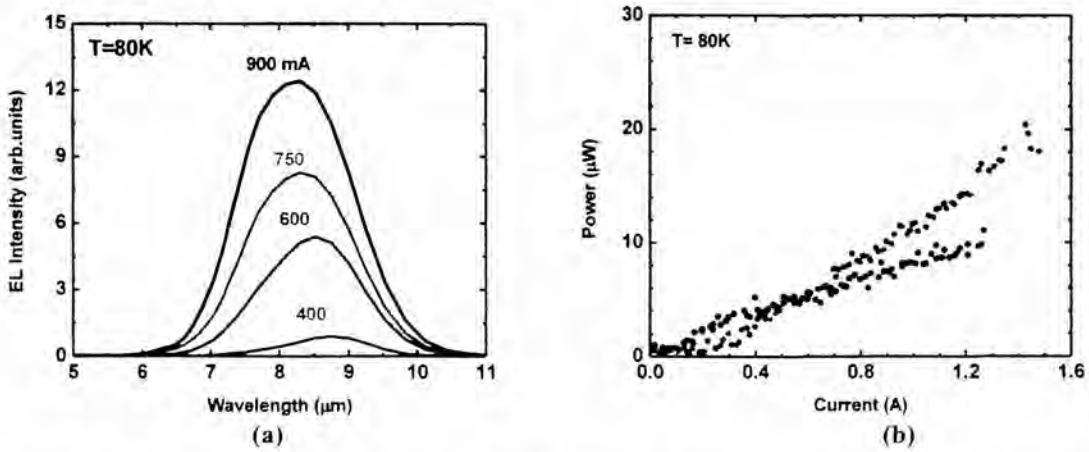

Figure 7. Electroluminescence spectra (a) and power dependences on current (b) for the InAsSb heterostructures with 44 % Sb composition. The spectra in panel (a) correspond to the structure with a 3-μm active layer thickness. The blue and red symbols in panel (b) correspond to the heterostructures with different thickness of the active region, 1 and 3-μm, respectively.

4. BARRIER DETECTORS FOR LONG WAVE INRARED RANGE

We assessed the feasibility of the similar barrier heterostructures with bulk InAsSb alloys for the detection of long-wave infrared radiation. The top contact layer doping was replaced with Tellurium to resemble n-B-n type barrier detectors.

The depleted AlInSb barrier was grown lattice matched to InAsSb with 44 % Sb composition. The schematic band diagram of the heterostructure under bias is shown in Figure 8.

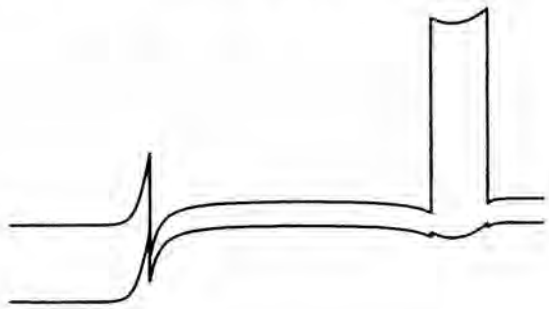

Figure 8. The schematic band diagram for the heterostructure with a bulk InAsSb absorber with 44 % of Sb composition. The AlInSb barrier was lattice-matched to the InAsSb absorber layer. The top contact layer was doped with Tellurium to a level of $n = 1\times10^{18}$ cm^{-3}.

For measurements of the absolute values of responsivity and external efficiency the heterostructures were processed with a window for incident radiation on top of the epilayer. The window opening was a square with a 400-μm side. The top metal contact layer was a square with a 600-μm side. The InAsSb contact layer outside the metal contact was removed down to the barrier layer by reactive ion etching. Silicon Nitride was used for isolation. No coating was deposited.

The external quantum efficiency (QE) spectra were obtained with FTIR spectrometry. The absolute values of the responsivity and the quantum efficiency, respectively, were obtained using a black body with the temperature of 800 °C.

In agreement with the expected band profiles the n-B-n device required a negative DC bias applied to the top contact to suppress the barrier for minority holes. The QE was increasing with bias until it reached a constant value at the bias of - 0.45 V. The QE spectra in Figure 9 are presented for the bias voltage of - 0.45 V for the temperatures of 80 and 150 K. The distortion of the QE spectra between λ = 5.5 and 8 μm are explained by atmospheric absorption. The QE increases monotonically with photon energy from λ= 10 μm at T = 80 K and from λ= 11 μm at T = 150 K. The absolute values of QE in the long wave infrared range are relatively high considering incomplete absorption in the relatively thin absorber. An increase of QE with temperature from T= 80 to 150 K at a particular wavelength is likely due to red shift of the energy gap with temperature. It showed that the carrier lifetime is not limited by Auger recombination, the diffusion length is sufficiently large compared to the absorber thickness and the QE is not limited by hole transport. It was concluded that QE for the long-wave infrared photodetectors based on the bulk InAsSb layers should benefit from increase of the absorber thickness.

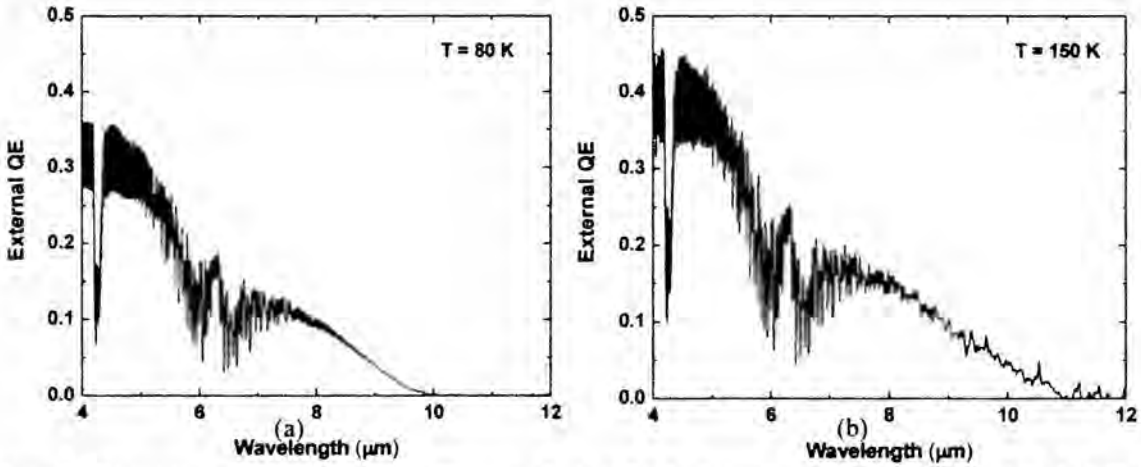

Figure 9. The spectra of external quantum efficiency obtained for the heterostructures with a 1-μm-thick InAsSb layers with Sb composition of 44 % at the temperatures of 80 K (a) and 150 K (b).

The I-V characteristics of the same InAsSb heterostructure measured up to room temperature under dark conditions are shown in Figure 10a. At the bias voltage of - 0.45 V the dark current density was 5×10^{-4} A/cm^2. Figure 10b presents the temperature dependence of the current measured at the bias voltage of - 0.45 V. The slope of the dependence taken in the temperature range from T= 100 to 200 K showed the activation energy of 124 meV nearly matching to the energy gap of the absorber.

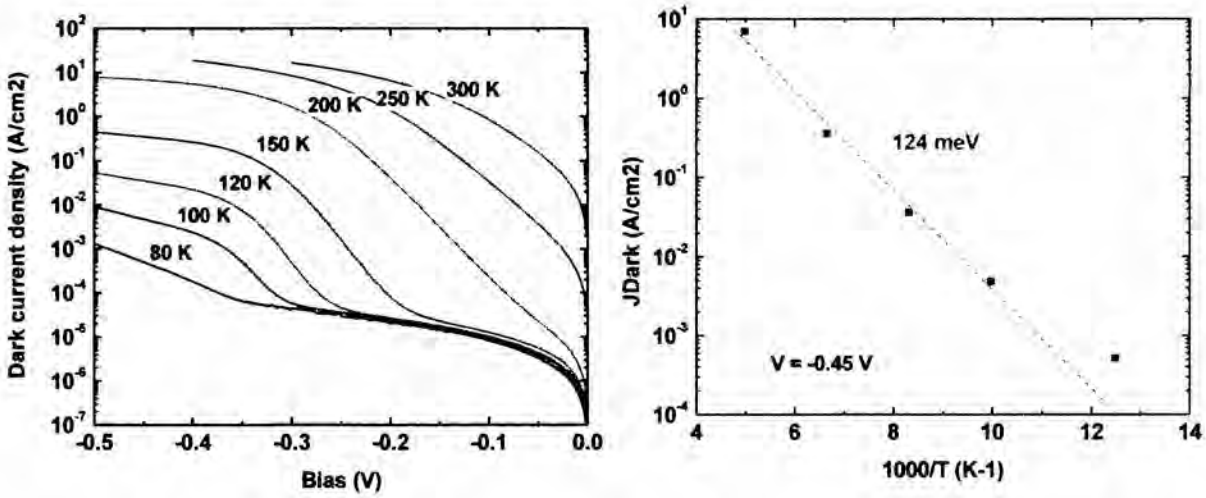

(a) (b)

Figure 10. (a) The current-voltage characteristics for the InAsSb/AlInSb heterostructure with 44 % Sb composition in the bulk InAsSb absorber measured from T= 80 K to 300 K; (b) Temperature dependence of the dark current for the bias voltage of -0.45 V. The dependence showed the activation energy of 124 meV in the temperature range from T= 100 to 200 K.

One can conclude that the barrier heterostructures with a 1-μm-thick bulk $InAsSb_{0.44}$ layer showed adequate light absorption and transport of minority holes across the absorber. The QE should benefit from increased absorber layer thicknesses. Future optimization of the composition and doping in the barrier layer should reduce the bias voltage. Optimization of the doping in the absorber layer is likely to reduce the dark current.

5. SUMMARY

It was demonstrated that the bulk InAsSb materials free of group-V ordering grown on metamorphic buffers are capable of encompassing the long wave infrared range at low temperatures. The characterization data obtained for unoptimized heterostructures suggests sufficiently large absorption and carrier lifetimes (long diffusion length) suitable for the development of infrared detectors and emitters with high quantum efficiencies. The carrier transport, including the transport of minority holes, is adequate for the development of detectors and emitters with increased active layer thickness.

ACKNOWLEDGEMENTS

The work was supported by US Army Research Office through grants W911NF1110109 and W911NF1220057 and by US National Science Foundation through grant DMR1160843.

REFERENCES

[1]. Osbourn G. C., "InAsSb strained-layer superlattices for long wavelength detector applications", *J. Vac. Sci. Technol. B*, **2**, 176 (1984).

[2]. Lee G. S., Lo Y., Lin Y. F., Bedair S. M., and Laidig W. D., "Growth of $InAs_{1-x}Sb_x$ (0<x<1) and InSb-InAsSb superlattices by molecular beam epitaxy", *Appl. Phys. Lett.*, **47**, 1219 (1985).

[3]. Yen M. Y., People R., Wecht K. W., and Cho A. Y., "Longwavelength photoluminescence of $InAs_{1-x}Sb_x$ (0<x<1) grown by molecular beam epitaxy on (100) InAs", *Appl. Phys. Lett.*, **52**, 489 (1988).

[4]. Yen M. Y., People R., and Wecht K. W., "Long wavelength (3–5 and 8–12 μm) photoluminescence of $InAs_{1-X}Sb_X$ grown on (100) GaAs by molecular beam epitaxy", *J. Appl. Phys.*, **64**, 952 (1988).

[5]. Tsukamoto S., Bhattacharya P., Chen Y. C., and Kim J. H., "Transport properties of $InAs_xSb_{1-x}$ ($0 \leq x \leq 0.55$) on *InP* grown by molecular beam epitaxy", *J. Appl. Phys.*, **67**, 6819 (1990).

[6]. Bethea C. G. , Levine B. F., Yen M. Y., Cho A. Y., "Photoconductance measurements on $InAs_{0.22}Sb_{0.78}$/GaAs grown using molecular beam epitaxy", *Appl. Phys. Lett.*, **53**, 291 (1988).

[7]. Yen M. Y., Levine B. F., Bethea C. G., Choi K. K., and Cho A. Y., "Molecular beam epitaxial growth and optical properties of $InAs_{1-X}Sb_X$ in 8–12 μm wavelength range", *Appl. Phys. Lett.*, **50**, 927 (1987).

[8]. Fang Z. M., Ma K. Y., Jaw D. H., Cohen R. M., and Stringfellow G. B., "Photoluminescence of InSb, InAs, and InAsSb grown by organometallic vapor phase epitaxy", *J. Appl. Phys.*, **67**, 7034 (1990).

[9]. Kurtz S. R., Dawson L. R., Biefeld R. M., Follstaedt D. M., and Doyle B. L., "Ordering-induced band-gap reduction in $InAs_{1-x}Sb_x$ ($x \cong 0.4$) alloys and superlattices", *Phys. Rev. B*, **46**, 1909 (1992).

[10]. Jen H. R., Ma K. Y., and Stringfellow G. B., "Long-range order in InAsSb", *Appl. Phys. Lett.*, **54**, 1154 (1989).

[11]. Dawson L. R., "Summary Abstract: Molecular beam epitaxial growth of InAsSb alloys and superlattices", *J. Vac. Sci. Techn. B*, **4**, 598 (1986).

[12]. Kurtz S. R., Osbourn G. C., Biefeld R. M., Dawson L. R., and Stein H. J., "Extended infrared response of InAsSb strained layer superlattices", *Appl. Phys. Lett.*, **52**, 831 (1988).

[13]. Kurtz S. R., Dawson L. R., Zippenan T. E., Whaley R. D. Jr, "High-Detectivity (> 1 x 10^{10} $cmHz^{1/2}/W$) InAsSb Strained-Layer Superlattice Photovoltaic Infrared Detector", *IEEE Electr. Device Lett.*, **11**, 54 (1990).

[14]. Zhang Y.-H., Lew A., Yu E., Chen Y., "Microstructural properties of InAs/InAsSb superlattices and InAsSb ordered alloys grown by molecular beam epitaxy", *J.Crystal Growth*, 175/176, 833 (1997).

[15]. Besikci C., Ozer S., Van Hoof C., Zimmermann L., John J., and Merken, P., Characteristics of $InAs_{0.8}Sb_{0.2}$ photodetectors on GaAs substrates, *Semicond. Sci. Technol.*, **16**, 992 (2006).

[16]. Liu P.-W., Tsai G., Lin H. H., Krier A., Zhuang Q. D., and Stone M., "Photoluminescence and bowing parameters of InAsSb/InAs multiple quantum wells grown by molecular beam epitaxy", *Appl. Phys. Lett.*, **89**, 201115 (2006).

[17]. Wu B.-R., Liao C., and Cheng K. Y., "High quality InAsSb grown on InP substrates using AlSb/AlAsSb buffer layers", *Appl. Phys. Lett.*, **92**, 062111 (2008).

[18]. Maimon S. and Wicks G.W., "nBn detector, an infrared detector with reduced dark current and higher operating temperature", *Appl.Phys.Lett.*, **89**, 151109 (2006).

[19]. Klipstein P.C., "xBn barrier photodetectors for high sensitivity and high operating temperature infrared sensors", *Infrared Technology and Applications, XXXIV*, ed. by B. J. Andresen, G. F. Fulop, P. R. Norton, *Proc. of SPIE*, **6940**, 694002U (2008).

[20]. Lackner D., Pitts O. J., Steger M., Yang A., Thewalt M. L. W. and Watkins S. P., "Strain balanced InAs/InAsSb superlattice structures with optical emission to 10 μm", *Appl. Phys. Lett.*, **95**, 081906 (2009).

[21]. Belenky G., Donetsky D., Kipshidze G., Wang D., Shterengas L., Sarney W. L., and Svensson S. P., "Properties of unrelaxed $InAs_{1-X}Sb_X$ alloys grown on compositionally graded buffers", *Appl. Phys. Lett.*, **99**, 141116 (2011).

[22]. Steenbergen E.H.,. Connelly B.C, Metcalfe G.D., Shen H., Wraback M., Lubyshev D., Qiu Y., Fastenau J.M., Liu A.W.K., Elhamri S., Cellek O.O. and Zhang Y.-H., "Significantly improved minority carrier lifetime observed in a long-wavelength infrared III-V type-II superlattice comprised of InAs/InAsSb", *Appl. Phys. Lett.*, **99**, 251110 (2011).

[23]. Svensson S. P., Sarney W. L., Hier H., Lin Y., Wang D., Donetsky D., Shterengas L., Kipshidze G. and Belenky G., "Band gap of $InAs_{1-x}Sb_x$ with native lattice constant", *Phys. Rev. B*, 86, 245205 (2012).

[24]. Plis E., Myers S., Kutty M. N., Mailfert J., Smith E.P., Johnson S., and Krishna S., Lateral diffusion of minority carriers in InAsSb-based nBn detectors, *Appl. Phys. Lett.*, 97, 123503 (2010).

[25]. Olson B. V., Shaner E. A., Kim J. K., Klem J. F., Hawkins S. D., Murray L. M., Prineas J. P., Flatté M. E., and Boggess T. F.,' "Time-resolved optical measurements of minority carrier recombination in a mid-wave infrared InAsSb alloy and InAs/InAsSb superlattice", *Appl. Phys. Lett.*. 101, 092109 (2012).

[26]. Donetsky D., Belenky G., Svensson S. P., and Suchalkin S., "Minority carrier lifetime in type-2 InAs–GaSb strained-layer superlattices and bulk HgCdTe materials", *Appl. Phys. Lett.*, 97, 052108 (2010).

[27]. Connelly B. C., Metcalfe G. D., Shen H., Wraback M., "Direct minority carrier lifetime measurements and recombination mechanisms in long-wave infrared type II superlattices using time-resolved photoluminescence ", *Appl. Phys. Lett.*, **97**, 251117 (2010).

[28]. Hakala M., Puska M. J., and Nieminen R. M., "Native defects and self-diffusion in GaSb", *J. Appl. Phys.*, **91**, 4988 (2002).

[29]. Svensson S. P., Donetsky D., Wang D., Hier H., Crowne F. J., Belenky G., "Growth of type II strained layer superlattice, bulk InAs and GaSb materials for minority lifetime characterization", *J. Cryst. Growth*, **334**, 103 (2011).
[30]. Wang D., Lin Y., Donetsky D., Shterengas L., Kipshidze G., Belenky G., Sarney W. L., Hier H., and Svensson S. P., "Unrelaxed bulk InAsSb with novel absorption, carrier transport and recombination properties for MWIR and LWIR photodetectors", Infrared Technology and Applications, XXXVIII, ed. by B. J. Andresen, G. F. Fulop, P. R. Norton, *Proc. of SPIE*, **8353**, 835312 (2012).
[31]. Kim H. S., Cellek O. O., Lin Zh.-Y., He Zh. –Y., Zhao X.-H., Liu S., Li H., and Zhang Y.-H., "Long-wave infrared nBn photodetectors based on InAs/InAsSb type-II superlattices", *Appl. Phys. Lett.*, **101**, 161114 (2012).
[32]. Kipshidze G., Hosoda T., Sarney W. L., Shterengas L., and Belenky G., "High-power 2.2-μm diode lasers with metamorphic arsenic-free heterostructures", *IEEE Photon. Technol. Lett.*, **23**, 317 (2011).
[33]. Lin Y., Wang D., Donetsky D., Shterengas L., Kipshidze G., Belenky G., Svensson S. P., Sarney W. L., Hier H. S., "Conduction- and Valence-Band Energies in Bulk $InAs_{1-x}Sb_x$ and Type II $InAs_{1-x}Sb_x$/InAs Strained-Layer Superlattices", *J. of Electron. Mater.*, **42**, 918 (2012).
[34]. Belenky G., Wang D., Lin Y., Donetsky D., Kipshidze G., Shterengas L., Westerfeld D., Sarney W.L., and Svensson S. P., "Metamorphic InAsSb/AlInAsSb heterostructures for optoelectronic applications", *Appl. Phys. Lett.*, **102**, 111108 (2013).